IL NUOVO CIMENTO **47 C** (2024) 287
DOI 10.1393/ncc/i2024-24287-4

COMMUNICATIONS: SIF Congress 2023

Status of the MEG II experiment: Searching for cLFV

ANTOINE VENTURINI(1)(2) on behalf of the MEG II COLLABORATION

(1) *INFN Sezione di Pisa - Largo B. Pontecorvo 3, 56127 Pisa, Italy*
(2) *Dipartimento di Fisica dell'Università di Pisa - Largo B. Pontecorvo 3, 56127 Pisa, Italy*

received 30 January 2024

Summary. — We report the first results of the MEG II experiment on the search for the $\mu \to e\gamma$ decay using the dataset collected in 2021. No evidence for this decay has been found: an upper limit on the branching ratio has been set to $\mathcal{B}(\mu^+ \to e^+\gamma) < 7.5 \times 10^{-13}$ (90% CL). Combination of this result with the previous limit set by MEG experiment yields the most stringent limit on this charged lepton flavor violating decay: $\mathcal{B}(\mu \to e\gamma) < 3.1 \times 10^{-13}$ (90% CL).

1. – Introduction

In the Standard Model (SM) of Particle Physics with massive neutrinos charged lepton flavour-violating (cLFV) processes, like the $\mu \to e\gamma$ decay, are strongly suppressed, with expected branching ratios of order $\mathcal{O}(10^{-50})$. Since the SM expected values are so tiny, any experimental evidence of excesses of cLFV processes would be a clear proof for New Physics beyond the SM; in fact, cLFV processes are predicted to possibly have observable rates in most SM extensions, further motivating the interest in experiments searching for them because they are very sensitive tools to investigate the Physics beyond the SM. An overview on the theoretical and experimental status of cLFV search is provided in [1] and references therein.

The MEG II Collaboration searches for the $\mu^+ \to e^+\gamma$ decay at the Paul Scherrer Institut (PSI) muon beam facility. Its goal is to improve the sensitivity on the branching ratio of this decay to $\mathcal{B}(\mu^+ \to e^+\gamma) < 6 \times 10^{-14}$ (90% CL), an order of magnitude better than the sensitivity of MEG experiment, which hields the present best limit $\mathcal{B}(\mu^+ \to e^+\gamma) < 4.2 \times 10^{-13}$ (90% CL) [2]. Here we summarize the principal aspects of the MEG II experiment and reports its first results on the search for the $\mu \to e\gamma$ decay using the 2021 dataset. The details about this measurement can be found in [3].

2. – MEG II experimental apparatus

The MEG II experiment is located downstream the πE5 beam line at PSI delivering a continuous beam of positive muons with an average momentum of 28 MeV/c that can be stopped in a thin plastic target at the center of the apparatus. A signal from the $\mu^+ \to e^+\gamma$ decay has a clear signature in the center-of-mass frame (in MEG II this

coincides with the laboratory frame): a positron (e^+) and a photon (γ) are emitted at the same time ($t_{e\gamma} \equiv t_e - t_\gamma = 0$) in opposite directions ($\Theta_{e\gamma} \equiv$ angle between directions of flight $= \pi$) and with almost the same energy ($E_{e^+} \approx E_\gamma \approx m_\mu c^2/2 \approx 52.83$ MeV).

MEG II's detector system, which mainly consists of a magnetic spectrometer and a photon detector (fig. 1), was optimized to improve the resolutions for e^+ and γ measurements, essential to distinguish a signal event from the experimental background. This latter has two sources [4]: radiative muon decays (RMD) $\mu^+ \to e^+\gamma\nu\overline{\nu}$ and accidental coincidences (the dominant background) between high energy e^+ and γ. Detectors are built to attain optimal performances while coping with the high muon rate, which is essential to have large statistics (the beam rate was varied during 2021 data-taking between 2 and 5×10^7 $\mu^+ s^{-1}$). More details about MEG II apparatus (and calibrations) can be found in [5].

The magnetic spectrometer is composed of three elements: e^+s are bent inside a spatially-varying magnetic field created by the COBRA (COnstant Banding RAdius) superconducting magnet and are tracked by a highly-segmented and ultra-low cylindrical drift chamber [6]. The pixelated Timing Counter detector [7] (pTC), composed of 512 scintillating tiles readout by SiPMs, provides precise e^+s timing and prompt information about their trajectory, both used at the trigger level.

The photon detector uses 900 liters of liquid xenon as scintillating material (high purity, high light yield, fast scintillation). The scintillation light is readout by 4092 SiPMs [8] on the entrance face of the detector for good position resolution of the interaction vertex. The sides and back of the detector volume are instrumented with 668 PMTs.

The MEG II experiment profits also of an auxiliary detector (the Radiative Decay Counter, RDC) composed of scintillating bars and a LYSO calorimeter to tag low energy e^+s which may coincide with energetic γs: this helps in identifying RMD decays which, in coincidence with an energetic e^+, can contribute to the accidental background, therefore reducing the background contamination.

The trigger and data-acquisition compose an integrated system in MEG II [9, 10]: a sophisticated trigger using FPGAs selects candidate signal events based on online estimates of $t_{e^+\gamma}$, E_γ and $\Theta_{e^+\gamma}$; for each triggered event the waveform of each detector channel (more than 9000) is digitized for precise offline reconstruction.

Performances of the detector system are listed in table I.

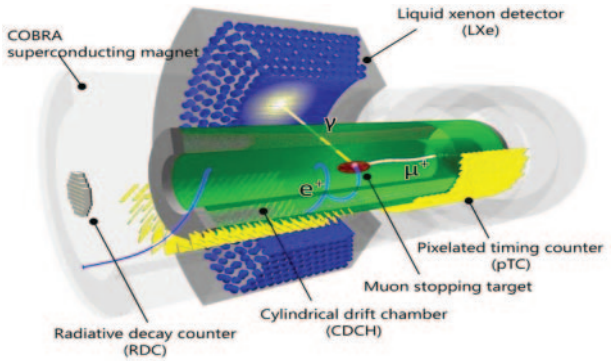

Fig. 1. – MEG II detector scheme with a simulated $\mu^+ \to e^+\gamma$ event. Modified from [5].

TABLE I. – *Detectors' resolutions and efficiencies at* 3×10^7 $\mu^+ s^{-1}$ *beam intensity. Derived from* [5].

Resolutions				Efficiencies		
σ_{E_γ}	σ_{p_e}	$\sigma_{t_{e\gamma}}$	$\sigma_{\Theta_{e\gamma}}$	ϵ_{e^+}	ϵ_γ	$\epsilon_{Trigger}$
1.8–2.0% @ 52.83 MeV	89 keV	78 ps	14.1 rad	67%	62%	80%

3. – Analysis strategy and results with 2021 data

Analysis strategy. – The MEG II experiment adopts a blind analysis approach to analyze the data. Events inside a "blinding box" ($48.0 < E_\gamma < 58.0$ MeV and $|t_{e^+\gamma}| < 1$ ns) are hidden until the likelihood fit function ($\mathcal{L}$) has been defined. $\mathcal{L}$ is the product of each event's probability density function (PDF): PDFs are built analyzing data in the sidebands outside the blinding box and using Monte Carlo simulations; they are functions of the observables $\vec{x_i} = \{E_\gamma,\ E_{e^+},\ t_{e^+\gamma},\ \Theta_{e^+\gamma}$ (or $\theta_{e^+\gamma},\ \phi_{e^+\gamma}$, which are the azimuthal and polar projection of $\Theta_{e^+\gamma}$, as defined in [3]), $t_{RDC} - t_{LXe},\ E_{RDC}, n_{pTC}\}$ (the number of hits in the pTC). $\mathcal{L}$ is used to perform an unbinned maximum likelihood fit of data inside an analysis region([1]) to extract a confidence interval for the expected number of signal events, N_{sig}. Confidence intervals for N_{sig} are built following the Feldman-Cousins prescription using the profile likelihood ratio ordering [11].

The extended likelihood is

$$\mathcal{L}(N_{sig},\ N_{RMD},\ N_{ACC},\ x_T) = \frac{e^{-(N_{sig}+N_{RMD}+N_{ACC})}}{N_{obs}!} C(N_{RMD},\ N_{ACC},\ x_T)$$
$$\times \prod_{i=1}^{N_{obs}} (N_{sig} Sig(\vec{x_i}) + N_{RMD} RMD(\vec{x_i}) + N_{ACC} ACC(\vec{x_i})),$$

where C is the product of the gaussian constraints on nuisance parameters (the number of background events N_{RMD} and N_{ACC} and the target position x_T) and $Sig,\ RMD,\ ACC$ are the PDFs of the signal and the background, respectively.

The branching ratio is derived using $\mathrm{B}(\mu \to e\gamma) = N_{sig}/N_\mu$, N_μ being the total number of measured muons in the experiment.

Results. – In 2021, during the first physics run, a total of 1.04×10^{14} μ^+ were stopped on the MEG II target, which yields an estimated normalization factor of $N_\mu = (2.64 \pm 0.12) \times 10^{12}$. The expected sensitivity $\mathcal{S}_{90}$ (see footnote [2]) on $\mathcal{B}(\mu^+ \to e^+\gamma)$ with 2021 data was estimated to be $\mathcal{S} = 8.8 \times 10^{-13}$. After unblinding of 2021 data, the likelihood fit was performed and yielded no evidence for the $\mu^+ \to e^+\gamma$ decay: the 90% CL upper limit of the branching ratio is $\mathcal{B}_{90}(\mu^+ \to e^+\gamma) < 7.5 \times 10^{-13}$. In fig. 2 we show

([1]) The analysis region envelops the region where a signal event is expected and is defined by $48 < E_\gamma < 58$ MeV; $52.2 < E_{e^+} < 53.5$ MeV; $|t_{e^+\gamma}| < 0.5$ ns; $|\phi_{e^+\gamma}| < 40$ mrad; $|\theta_{e^+\gamma}| < 40$ mrad.

([2]) Defined as the median of the distribution of 90% CL upper limits computed for 1000 Monte Carlo pseudo-experiments with null-signal hypothesis.

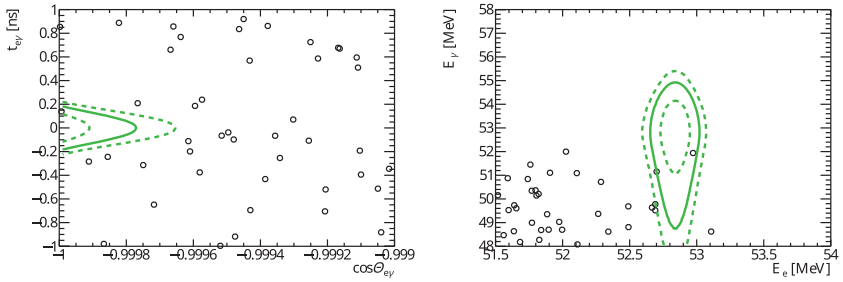

Fig. 2. – Distributions of events inside (part of) the signal region: (left) $\cos\Theta_{e^+\gamma} - t_{e^+\gamma}$ plane; right) $E_{e^+} - E_\gamma$ plane. Signal PDFs contours (for 1, 1.64, 2 σ) are drawn with green lines.

the event distribution inside the analysis region. No event falls inside the $2-\sigma$ signal region. The estimate for $\mathcal{B}_{90}$ is compatible with that obtained from a second independent analysis which uses a "constant PDF" likelihood function.

The upper limit can be combined with the MEG result to improve present limits on the $\mu \to e\gamma$ decay. Using the product of the likelihood functions from MEG II and MEG, the 90% CL upper limit is determined as the branching ratio that matches the value $-\log\mathcal{L} = 1.6$ ([3]). The combined sensitivity is $\mathcal{S}_{90} = 4.3 \times 10^{-13}$ and the combined branching ratio is

$$\mathcal{B}_{90}(\mu^+ \to e^+\gamma) = 3.1 \times 10^{-13}.$$

4. – Conclusions

In 2021, the MEG II Collaboration terminated the commissioning of the detector system and collected a seven-week long period of physics data in search for the cLFV decay $\mu^+ \to e^+\gamma$. A blinded, maximum-likelihood analysis found no evidence of this decay, setting the most stringent upper limit on $\mathcal{B}(\mu^+\gamma \to e^+\gamma)$ up to date. With the MEG II experiment planning to take data until 2026, the goal sensitivity of $\mathcal{S}_{90} = 6 \times 10^{-14}$ is in reach and will improve further our knowledge in the sector of cLFV.

REFERENCES

[1] Calibbi L. and Signorelli G., *Riv. Nuovo Cimento*, **41** (2018) 71.
[2] Baldini A. M. *et al.*, *Eur. Phys. J. C*, **76** (2016) 1.
[3] Afanaciev K. *et al.*, arXiv:2310.12614 (2024).
[4] Kuno Y. and Okada Y., *Rev. Mod. Phys.*, **73** (2001) 151.
[5] Afanaciev K. *et al.*, arXiv:2310.11902 (2024).
[6] Baldini A. M. *et al.*, arXiv:2310.12865 (2023).
[7] Nishimura M. *et al.*, *Nucl. Instrum. Methods A*, **958** (2020) 162785.
[8] Ieki K. *et al.*, *Nucl. Instrum. Methods A*, **925** (2019) 148.
[9] Galli L. *et al.*, *Nucl. Instrum. Methods A*, **936** (2019) 399.
[10] Francesconi M. *et al.*, *Nucl. Instrum. Methods A*, **1045** (2023) 167542.
[11] Feldman G. J. and Cousins R. D., *Phys. Rev. D*, **57** (1998) 3873.